Slug (SNAI2) Down-Regulation by RNA Interference Facilitates Apoptosis and Inhibits Invasive Growth in Neuroblastoma Preclinical Models

Roberta Vitali,[1] Camillo Mancini,[1] Vincenzo Cesi,[1] Barbara Tanno,[1] Mariateresa Mancuso,[1] Gianluca Bossi,[2] Ying Zhang,[5] Robert V. Martinez,[5] Bruno Calabretta,[6] Carlo Dominici,[3,4,7] and Giuseppe Raschellà[1]

Abstract

Purpose: We assessed the relevance of Slug (SNAI2) for apoptosis resistance and invasion potential of neuroblastoma cells *in vitro* and *in vivo*.

Experimental Design: We evaluated the effect of imatinib mesylate on invasion and analyzed the genes modulated by imatinib mesylate treatment in neuroblastoma cells. Slug expression, inhibited by imatinib mesylate treatment, was knocked down in neuroblastoma cells by RNA interference, and the effects on invasion and apoptosis were evaluated *in vitro*. A pseudometastatic model of neuroblastoma in severe combined immunodeficient mice was used to assess the effects of Slug silencing alone or in combination with imatinib mesylate treatment on metastasis development.

Results: Microarray analysis revealed that several genes, including Slug, were down-regulated by imatinib mesylate. Slug expression was detectable in 8 of 10 human neuroblastoma cell lines. Two Slug-expressing cell lines were infected with a vector encoding a microRNA to Slug mRNA. Infected cells with reduced levels of Slug were tested for the expression of apoptosis-related genes (p53, Bax, and Bcl-2) identified previously as Slug targets. Bcl-2 was down-regulated in Slug-interfered cells. Slug down-regulation increased sensitivity to apoptosis induced by imatinib mesylate, etoposide, or doxorubicin. Invasion of Slug-silenced cells was reduced *in vitro*. Animals injected with Slug-silenced cells had fewer tumors than controls and the inhibition of tumor growth was even higher in animals treated with imatinib mesylate.

Conclusions: Slug down-regulation facilitates apoptosis induced by proapoptotic drugs in neuroblastoma cells and decreases their invasion capability *in vitro* and *in vivo*. Slug inhibition, possibly combined with imatinib mesylate, may represent a novel strategy for treatment of metastatic neuroblastoma.

Formation of secondary tumors (metastasis) in organs distant from the primary neoplasm is the leading cause of death in cancer patients (1). Along the metastatic route, tumor cells invade the tissues surrounding the primary tumor, enter either the lymphatics or the bloodstream, survive and eventually arrest in the circulation, extravasate into a tissue, and grow at the distant site (2). To fulfill these tasks, cancer cells must undergo profound and interconnected changes that modify their morphology and function. At molecular level, these changes are driven by the modulation of several genes whose identity is not yet completely known. Schematically, the picture emerging from recent data suggests that tumor cells transit to mesenchymal phenotype (3, 4), up-regulate specialized proteases (5), and expose membrane receptors that allow them to home to permissive locations (6). In addition, metastatic cells also need to activate angiogenesis at distant sites (7) by releasing angiogenic factors. A growing body of evidence has pointed out to the relevance of several distinct families of transcription factors able to mediate the changes required for local invasion, the initial and critical step to metastasis (4).

Neuroblastoma is the most common extracranial childhood tumor with a prevalence of 1 case in 7,000 live births (8). Neuroblastoma derives from cells of the sympatoadrenal lineage of the neural crest that arrest at some stage of their differentiation (8). Approximately 40% of newly diagnosed patients present with localized disease that, in most cases, is easily curable or regresses spontaneously (9). By contrast, ~50% of patients present with metastatic disease associated

Authors' Affiliations: [1]Section of Toxicology and Biomedical Sciences, ENEA Research Center Casaccia; [2]Department of Experimental Oncology, Regina Elena Cancer Institute; [3]Department of Pediatrics, La Sapienza University; [4]Laboratory of Oncology, Bambino Gesù Children's Hospital, Rome, Italy; [5]Department of Biological Technologies, Wyeth Research, Cambridge, Massachusetts; [6]Kimmel Cancer Center, Thomas Jefferson University, Philadelphia, Pennsylvania; and [7]Division of Child Health, School of Reproductive and Developmental Medicine, Liverpool University, Liverpool, United Kingdom

Received 12/19/07; revised 2/22/08; accepted 3/5/08.

Grant support: Fondazione Italiana per la Lotta al Neuroblastoma (G. Raschellà), Italian Ministry of Health and Associazione per la Lotta contro i Tumori Infantili (C. Dominici), and National Cancer Institute grant RO1 CA95111 (B. Calabretta). R. Vitali is a fellow of Fondazione Italiana per la Lotta al Neuroblastoma.

The costs of publication of this article were defrayed in part by the payment of page charges. This article must therefore be hereby marked *advertisement* in accordance with 18 U.S.C. Section 1734 solely to indicate this fact.

Requests for reprints: Giuseppe Raschellà, Section of Toxicology and Biomedical Sciences, ENEA Research Center Casaccia, Via Anguillarese, 301-00123 Rome, Italy. Phone: 39-0630483172; Fax: 39-0630486559; E-mail: raschella@casaccia.enea.it.

doi:10.1158/1078-0432.CCR-07-5210

with very poor outcome despite intensive therapeutic protocols including high-dose chemotherapy and myeloablative regimens followed by hematopoietic rescue (10). A peculiar type of neuroblastoma, so called stage 4S, characterized by a small primary tumor and a widespread involvement of liver, skin, or bone marrow that almost always spontaneously regress (11), accounts for ~5% to 7% of the cases. The clinical heterogeneity of neuroblastoma is mirrored by the complexity of the genetic features that characterize this tumor (8). Apart from MYCN genomic amplification, the alteration more consistently associated with poor outcome (12), several other genetic changes are currently used to better define prognosis (9).

The neuroectodermal origin of neuroblastoma suggests that this tumor can spread from the primary site using mechanisms similar to those operating during the formation and delamination of the embryonic neural crest (13). Thus, the same gene(s) that are relevant for the migration of neural crest cells may also play a role in the acquisition of the invasive phenotype of neuroblastoma cells.

Imatinib mesylate (Gleevec, Glivec, STI-571) is a soluble small-molecule successfully used to treat chronic myelogenous leukemia for its inhibitory activity of the BCR-ABL tyrosine kinase (14). Subsequently, the use of imatinib mesylate has been extended to gastrointestinal stromal tumors where it acts by inhibiting c-Kit (15). We and others showed that imatinib mesylate is also active in inhibiting neuroblastoma growth *in vitro* and *in vivo* (16–18). Of interest, other studies confirming the antiproliferative activity of imatinib mesylate in neuroblastoma have suggested that the drug's activity is not strictly dependent on c-Kit inhibition (19, 20). It should be also noted that a recent clinical trial on refractory or relapsed childhood solid tumors, including neuroblastoma, described imatinib mesylate as a single agent at a dose of 440 mg/m^2/d shows little or no activity (21).

In this study, we evaluated the effect of imatinib mesylate in reducing invasion and metastasis in neuroblastoma cells. By applying microarray analysis, we identified the transcription factor Slug (SNAI2; ref. 4) as a target of imatinib mesylate. By inhibiting Slug expression by RNA interference, we found that reduced Slug levels decreased survival and invasion in neuroblastoma. Finally, in a pseudometastatic model of neuroblastoma in mice, we showed an additive effect of Slug silencing and imatinib mesylate treatment in reducing the metastatic burden. These data suggest that Slug is a relevant gene for regulation of the metastatic potential of neuroblastoma cells and that strategies combining imatinib mesylate treatment and Slug inhibition may be suitable as a treatment of metastatic neuroblastoma.

Materials and Methods

Cell lines. Human neuroblastoma cell lines SK-N-BE2c, SK-N-BE, SK-N-AS, SH-EP, KCNR, ACN, RN-GA, GI-CA-N, LAN-5, and HTLA-230 were kept in culture as described previously (16).

Reagents. Imatinib mesylate was provided by Novartis Pharma, etoposide by Bristol-Myers Squibb, and doxorubicin by Pharmacia.

Microarray analysis. Total RNA was extracted from cells seeded on Matrigel-coated dishes (BD Biosciences) using RNeasy spin columns (Qiagen) according to the manufacturer's instructions. Double-stranded cDNA was synthesized starting with 5 μg total RNA using the SuperScript System (Invitrogen). The cDNA was purified by filtration through Multiscreen filter plate (Millipore) and transcribed *in vitro* using T7 RNA polymerase (Epicenter) and biotinylated nucleotides (Perkin-Elmer Life Sciences). Hybridization buffer containing the spike pool reagent was added to each of the fragmented cRNA mixtures and each sample was hybridized to the Human Genome U133 2.0 array (Affymetrix) at 45°C for 18 h as recommended by the manufacturer. The hybridized chips were washed and stained using Affymetrix Fluidics Station 450 and the EukGE-WS2v4_450 protocol as recommended by the manufacturer. The staining was done using streptavidin-phycoerythrin conjugate (Molecular Probes) followed by biotinylated antibody against streptavidin (Vector Laboratories) and then streptavidin-phycoerythrin. The chips were scanned using an Affymetrix GeneChip Scanner and .cel files were generated with Affymetrix Microarray Suite 5.0 software. Using normalized data, after removing lowly expressed genes (those with a signal value below 43) and those that were consistently called absent "A," we imposed a nonstringent 1.1-fold change between imatinib mesylate–treated and untreated samples. A *t* test was done, and qualifiers with a $P \leq 0.05$ were then subjected to false discovery testing to select qualifiers with a false discovery rate ≤ 25%. These analyses were independently done on expression data from both GI-CA-N and HTLA-230. Using these criteria, a total of 21 qualifiers were regulated by imatinib mesylate in both cell lines. Slug was represented by one of these qualifiers.

Quantitative real-time PCR. Total RNA was extracted by RNeasy extraction kit (Qiagen) and reverse transcribed according to standard protocols. Real-time PCR was carried out using an ABI PRISM 7000 Sequence Detection System (Applied Biosystems). TaqMan technology, the Assays-On-Demand kit (Hs00161904_m1), for human Slug was used. TaqMan predeveloped kit part 4326315E for the human β-actin was used to normalize. Reactions were run in triplicate in two independent experiments.

Retrovirus/lentivirus vectors and infections. Retroviral constructs for human Slug were generated by cloning the full-length cDNA of human Slug obtained by reverse transcriptase-PCR into the pBabe-puro vector system using standard techniques. Slug sequence was confirmed by dideoxysequencing.

Amphotropic retroviruses were created by transient cotransfection of vector DNA into Phoenix cells (22). Briefly, 4×10^6cells were seeded in 10-cm plates and the plates were cotransfected with 1.5 μg packaging plasmid pCMV-VSVG and 13.5 μg pBabe-puro-Slug or pBabe-puro vector by calcium phosphate precipitation. Transfection was carried out in the presence of 25 μmol/L chloroquine (Sigma). Viral supernatants were harvested 24 h post-transfection by centrifugation at 3,000 rpm for 5 min and supplemented with 5 μg/mL polybrene (Sigma) before infection. Viral supernatants were used to infect neuroblastoma cell line LAN-5. Forty-eight hours after infection, cells were selected by puromycin (Sigma).

For microRNA-mediated inhibition, we used lentiviral vector pLKO-Slug3 obtained from Addgene, which encodes a microRNA directed against human Slug (23). In control infections, we used lentiviral vector pLKO-green fluorescent protein (GFP) that encodes a microRNA directed to GFP (23).

Lentiviruses were generated by transient cotransfection of DNA into 293FT cells. Briefly, 2.5×10^6 293FT cells were seeded in 10-cm plates and cotransfected with 21 μg of appropriate packaging plasmids pCMVd8.2/pCMV-VSVG (2.5:1) and 20 μg pLKO-Slug or pLKO-GFP vectors using calcium phosphate transfection kit (Invitrogen). After 6 to 8 h, medium was replaced with 6.0 mL complete medium supplemented with 1.0 mmol/L sodium pyruvate (Life Technologies). Recombinant lentivirus vectors were harvested 48 h later, centrifuged 5 min at 3,000 rpm, aliquoted, and stored at -80°C. Viral supernatants supplemented with 8 μg/mL polybrene (Sigma) were then used to infected neuroblastoma cell lines LAN-5 and HTLA-230, and 18 h after infection, the cells were selected by puromycin (Sigma).

Protein analysis. Cellular proteins were extracted and separated on SDS-PAGE gels, and Western blot analyses were carried out as described previously (24). Antibodies used were anti-Slug (G-18), anti-p53

(DO-1), anti-Bcl-2 (N-19), and anti-Bax (N-20) all from Santa Cruz Biotechnology; anti-β-actin (AC-15) from Sigma-Aldrich.

Tumor invasion in Matrigel-coated chambers. Cells were pretreated in complete medium supplemented with 10 μmol/L imatinib mesylate for 24 h before plating (1.25×10^5 per well) in the BD Matrigel invasion chambers (BD Biosciences). Mock treatments were carried out pretreating the cells in the same medium without imatinib mesylate. Medium in the upper chamber was supplemented with 5% FCS. In the lower chamber, FCS concentration was 10%. After 24 h, cells migrated into the lower chamber were stained and counted. Experiments were carried out in triplicate and repeated twice.

Flow cytometry. Cells (1×10^6) were harvested and the pellets were washed twice with PBS. Cells were then fixed in cold 70% ethanol added dropwise while vortexing gently. Fixed cells were kept overnight at 4°C. Cells were centrifuged and pellets were resuspended in 1 mL propidium iodide/RNase staining buffer (BD Biosciences). Reactions were incubated for 20 min at 4°C and protected from the light. Samples were analyzed by flow cytometry using a FACSCalibur flow cytometer (BD Biosciences). For each sample, at least 2×10^4 cells were analyzed. Cell cycle distribution was calculated by CellQuest software (BD Biosciences).

In vivo *studies.* For *in vivo* studies of metastasis suppression, 4-week-old CB-17/IcrHsd, severe combined immunodeficient mice (Harlan Italy) were fed *ad libitum* and kept in optimal hygienic conditions in a 12-h light/12-h dark cycle. On arrival, animals were kept in the animal facility for 1 week before starting the experiments. Animals were injected in the tail vein with 3×10^6 HTLA-230-pLKO-GFP or HTLA-230-pLKO-Slug cells. They were treated by oral gavage twice daily, 7 days/wk either with imatinib mesylate (200 mg/kg/d) dissolved in water (treated group) or with water (control group). The experiments were terminated 35 days after day 0. Animals were sacrificed by CO_2 inhalation, autopsy was carried out for macroscopic assessment of metastases, and organs were collected for histologic analysis. *In vivo* studies were approved by the Animal Care and Use Committee of the Department of Biotech-BAS, ENEA, and animal care was in accordance with local institutional guidelines. For histologic evaluation, paraffin-embedded tissues were cut in 7 μm sections and processed for H&E staining according to standard techniques. Evaluation of the percent of invaded areas was carried out using the software Image Tools for Windows version 3 (University of Texas Health Science Center).

Statistical analysis. Wilcoxon-Mann-Whitney exact test was applied to evaluate the statistical significance between the differences in the metastatic areas in different animal groups using GraphPad Prism 4 for Windows (GraphPad Software). Results are presented as mean ± SE. The level of significance was set at $P < 0.05$.

Results

***Imatinib mesylate inhibits invasion of neuroblastoma cells* in vitro.** Previous studies from our laboratory have shown that neuroblastoma cells are sensitive to imatinib mesylate most likely through inhibition of c-Kit-regulated survival and proliferative signals (16). In this study, we assessed the ability of imatinib mesylate to inhibit invasion of neuroblastoma cells *in vitro*. Human neuroblastoma cell lines (HTLA-230, LAN-5, SK-N-BE2c, and GI-CA-N) were seeded in Matrigel-coated invasion chambers in the absence or presence of imatinib mesylate (10 μmol/L). After 24 h, cells that migrated through the Matrigel barrier were stained and counted. Invasion was significantly inhibited by imatinib mesylate in all cell lines although to different extents (Fig. 1). In an attempt to elucidate the mechanisms by which imatinib mesylate suppresses invasiveness of neuroblastoma cells, we compared the transcriptional profile of neuroblastoma cells plated in Matrigel before and after treatment with imatinib mesylate (10 μmol/L for 6 h) by probing high-density microarrays with RNA from GI-CA-N and HTLA-230 cells. We only focused on differences in expression levels concordantly present in both cell lines. By setting a >1.1-fold variation threshold, we identified 21 qualifiers up-modulated or down-modulated by imatinib mesylate that correspond to the 19 known genes indicated in Table 1. Among these genes, Slug was selected for further studies because of its involvement in cell movement and survival of embryonic neural crest cells as well as in the epithelial-mesenchymal transition (EMT) that occurs at the beginning of the metastatic process (13).

Slug inhibition by RNA interference in neuroblastoma cells. Recent data indicate that Slug expression is relevant for melanoma metastasis (23). Because neuroblastoma shares the neuroctodermal origin with melanoma, we undertook experiments to assess whether Slug is involved in neuroblastoma invasion and metastasis. By Western blotting, expression of Slug was detected in 8 of 10 human neuroblastoma cell lines analyzed (Fig. 2A). Two neuroblastoma cell lines (HTLA-230 and LAN-5) that express Slug were selected for further studies. Slug expression, measured by quantitative real-time PCR, was significantly down-regulated by imatinib mesylate treatment (10 μmol/L for 6 h) in both cell lines (Fig. 2B).

To evaluate whether endogenous Slug plays any role in neuroblastoma cells, we down-regulated its expression in LAN-5 and HTLA-230 cells on infection with a lentiviral vector (pLKO-Slug) that encodes a microRNA targeting human Slug mRNA (23). Control infections were carried out with a vector (pLKO-GFP) encoding a microRNA directed against a segment of the coding sequence of GFP (23). Likewise, the effects of Slug overexpression were analyzed in LAN-5 cells retrovirally transduced with a vector (pBabe-Slug), which encodes human Slug. After puromycin selection, infected cells were tested for Slug expression by Western blotting. In pLKO-Slug-infected cells, Slug expression was barely detectable in both LAN-5 and HTLA-230 cells; by contrast, pLKO-GFP-infected cells showed

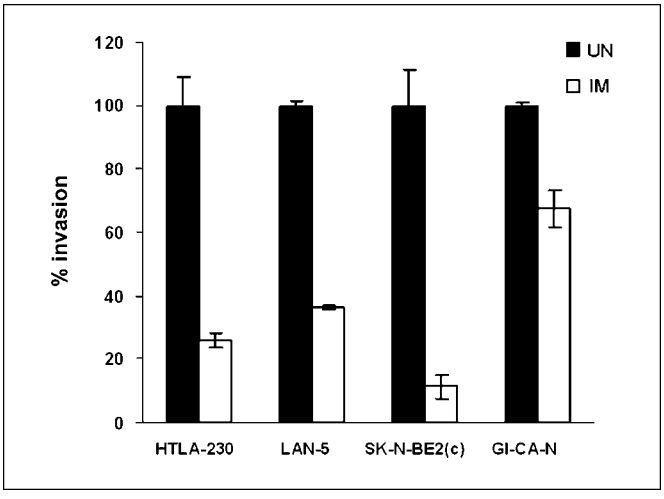

Fig. 1. Imatinib mesylate (*IM*) treatment inhibits invasion of human neuroblastoma cells in Matrigel-coated invasion chambers. Cells were seeded in the upper chamber in medium supplemented with 5% FCS, treated with imatinib mesylate (see details in Materials and Methods), or left untreated (*UN*). After 22 h, cells migrated in the lower chamber were stained and counted. In the lower chamber, medium supplemented with 10% FCS was used as chemoattractant. Invasion of the untreated cells was set to 100. Results are reported as percent migration ± SD compared with untreated cells. Experiments were carried out twice in triplicate.

Table 1. Genes whose expression is concordantly modulated by imatinib mesylate in GI-CA-N and HTLA-230 neuroblastoma cell lines

Identifier/descriptor	Symbol	GI-CA-N (imatinib mesylate/ untreated)	*t* test	HTLA-230 (imatinib mesylate/ untreated)	*t* test
Hypothetical gene supported by BC031266	NA	-1.40	0.04	-1.36	0.04
Polo-like kinase 2	PLK2	-1.42	0.01	-1.51	0.04
Calcitonin gene-related peptide-receptor component protein	RCP9	-1.48	0.04	-1.23	0.02
Embryo brain-specific protein	EBSP	-1.31	0.02	-1.35	0.01
Activin A receptor, type II	ACVR2	1.68	0.04	1.78	0.03
Mab-21-like 2	MAB21L2	1.15	0.00	1.19	0.04
Snail homologue 2	Slug (SNAI2)	-1.45	0.02	-1.18	0.04
Pleckstrin homology-like domain, family A, member 1	PHLDA1	-1.43	0.04	-3.04	0.04
Thymocyte protein thy28	THY28	-1.12	0.02	-1.28	0.01
Collaborates/cooperates with ARF	CARF	-1.76	0.01	-1.37	0.04
Phosphatidylinositol 4-kinase type-II β	PI4K2B	1.14	0.01	1.24	0.04
SH3 domain protein D19	EVE1	-1.33	0.00	-1.46	0.03
Tumor protein p53-inducible nuclear protein 1	TP53INP1	1.40	0.01	1.60	0.03
Chromosome 13 open reading frame 11	C13orf11	1.19	0.05	1.30	0.04
FLJ20758 protein	FLJ20758	-1.54	0.02	-1.38	0.00
Two pore segment channel 2	TPCN2	-1.47	0.04	-1.40	0.02
Anaphase-promoting complex subunit 1	ANAPC1	1.18	0.02	1.19	0.05
Chromosome 14 open reading frame 145	C14orf145	1.35	0.02	1.40	0.04
Hypothetical protein DKFZp761I2123	DKFZp761I2123	-1.43	0.02	-1.13	0.04

Slug levels similar to those in parental cells (Fig. 3A and B). pBabe-Slug cells expressed a higher amount of Slug compared with parental cells (Fig. 3A and B).

Because Slug has been shown to be involved in the control of apoptosis (25) and in the EMT that is linked to the acquisition of the invasive phenotype (4), we analyzed the expression of several Slug targets in Slug-silenced (pLKO-Slug) and Slug-overexpressing (pBabe-Slug) cells by immunoblotting. In LAN-5-pLKO-Slug and HTLA-230-pLKO-Slug cells, antiapoptotic Bcl-2 was down-regulated (Fig. 3A and B). By contrast, in Slug-overexpressing LAN-5-pBabe-Slug cells, Bcl-2 was up-regulated (Fig. 3A and B). Proapoptotic Bax was reported to be a Slug target in some cellular contexts (26), but in our analyses, its expression did not change in a consistent manner. p53 was up-regulated only in LAN-5-pLKO-Slug cells. In all cell lines, E-cadherin, a well-known target of Slug (27), was undetectable (data not shown).

We analyzed whether Slug levels affect cell proliferation by seeding Slug-silenced and Slug-overexpressing cells in normal culture conditions (medium + 10% FCS) and counting the cells at different time points. The growth rate was not significantly different ($P > 0.05$) in Slug-silenced HTLA-230-pLKO-Slug and LAN-5-pLKO-Slug cells compared with their respective controls (data not shown). Similarly, proliferation of LAN-5-pBABE-Slug cells was undistinguishable from that of control cells (data not shown). These results are consistent with recent data indicating that Slug does not affect proliferation of melanoma cells (23).

***Slug silencing inhibits invasion of neuroblastoma cells* in vitro.** We tested whether Slug knockdown affected the invasion capabilities of neuroblastoma cells by using an *in vitro* invasion assay. Cells were seeded in the upper part of a Matrigel-coated invasion chamber in a reduced (5%) FCS concentration. After 22 h, cells that migrated in the lower chamber containing a higher (10%) FCS concentration were stained and counted. In both Slug-silenced cell lines, invasion was significantly reduced (Fig. 4A and B). We also tested the effects of imatinib mesylate on the invasion capability of HTLA-230-pLKO-Slug and HTLA-230-pLKO-GFP cells. Compared with data obtained using the parental cell lines (see Fig. 1), imatinib mesylate–treated HTLA-230-pLKO-GFP and LAN-5-pLKO-GFP cells exhibited reduced invasion (Fig. 4A and B). Compared with untreated cells, no further decrease in invasion was observed in imatinib mesylate–treated HTLA-230- pLKO-Slug and LAN-5-pLKO-Slug cells (Fig. 4A and B). Of interest, LAN-5-pBABE-Slug cells that overexpress Slug showed an increased invasion capability; imatinib mesylate treatment reduced the invasion of these cells and the control LAN-5-pBABE-puro cells (Fig. 4C). Together, these data show that Slug modulates invasion of neuroblastoma cells *in vitro*.

Slug silencing and proapoptotic drug treatment cooperate in inducing apoptosis of neuroblastoma cells. Given the activity of Slug in cell survival through regulation of proapoptotic and antiapoptotic factors, we assessed the apoptosis susceptibility of Slug-silenced cells in the absence or presence of imatinib mesylate (24 μmol/L). We used this imatinib mesylate concentration because it is near the calculated IC_{50} for the two neuroblastoma parental cell lines (LAN-5 and HTLA-230; ref. 17) from which the Slug-silenced cells were derived. HTLA-230-pLKO-Slug and LAN-5-pLKO-Slug cells and their controls were grown in normal growth conditions (medium + 10% FCS) in the presence or absence of imatinib mesylate for different times (1, 2, and 3 days). At the end of each treatment, cells were fixed and stained with propidium iodide for flow cytometric analysis. Spontaneous (without imatinib mesylate) apoptosis (sub-G_1 peak) increased only in HTLA-230-pLKO-Slug cells compared with control HTLA-230-pLKO-GFP (Table 2). In Slug-silenced cell lines, apoptosis induced by imatinib mesylate was markedly increased at each time point ($P < 0.001$, χ^2 test), except after 1-day treatment of LAN-5-pLKO cells (Table 2). Thus, at least *in vitro*, simultaneous Slug down-regulation by RNA interference and imatinib mesylate treatment cooperate in

promoting apoptosis. In addition, we tested whether Slug silencing could also cooperate in inducing apoptosis with etoposide and doxorubicin, two drugs frequently used in standard therapeutic protocols for neuroblastoma. Both Slug-silenced cell lines (LAN-5-pLKO-Slug and HTLA-230-pLKO-Slug) showed significantly increased apoptosis ($P < 0.001$, χ^2 test) compared with controls at 1, 2, and 3 days of treatment (LAN-5-pLKO-Slug + doxorubicin) and at 1 and 2 days of treatment (LAN-5-pLKO-Slug + etoposide, HTLA-230-pLKO-Slug + etoposide, and HTLA-230-pLKO-Slug + doxorubicin; Table 2). These data suggest that Slug silencing can be usefully combined with apoptosis-inducing drugs to accelerate and/or maximize antitumor effect.

Effect of Slug silencing in an* in vivo *pseudometastatic model. The next step for the characterization of Slug function in neuroblastoma was to test the effect of Slug knockdown in animal models. Tail vein injection in severe combined immunodeficient mice provides a well-known pseudometastatic model for neuroblastoma (28). Because not all neuroblastoma cell lines develop tumors after i.v. injection in mice, we selected HTLA-230 cells because they are the most reliable model of neuroblastoma metastasis in mice (28). Severe combined immunodeficient mice were injected with 3×10^6 HTLA-230-pLKO-Slug (20 animals) or HTLA230-pLKO-GFP (20 animals) on day 0. On day 1, mice were divided in four groups of 10 animals each (HTLA-230-pLKO-Slug untreated, HTLA-230-pLKO-Slug + imatinib mesylate, HTLA230-pLKO-GFP untreated, and HTLA230-pLKO-GFP + imatinib mesylate) and imatinib mesylate treatment was started by oral gavage twice a day (total daily dose, 200 mg/kg) and continued for 21 days. Animals were sacrificed after the occurrence of the first death (day 35) and autopsy was carried out to remove organs and detect macrometastases. Autopsy showed a reduction of tumor cell burden in certain organs (adrenals, kidneys, liver, and lungs) in HTLA-230-pLKO-Slug untreated and HTLA-230-pLKO-Slug + imatinib mesylate groups. The major site for metastases was a pararenal area involved in 100% of the animals in HTLA230-pLKO-GFP untreated and HTLA230-pLKO-GFP + imatinib mesylate groups. Involvement of this pararenal area was reduced in HTLA-230-pLKO-Slug untreated and HTLA-230-pLKO-Slug + imatinib mesylate groups. Because the extent of pararenal involvement was correlated to the overall metastatic burden (data not shown), we analyzed the percentage of metastatic invasion in the major sagittal section of the kidney, pararenal area, and adrenal of each animal. From each group, histologic specimens were prepared and the largest sagittal section of each organ was evaluated using an image analysis software to measure the extent of tumor involvement. We plotted the percentage of the invaded areas to estimate the metastatic burden in each group of animals (Fig. 5A). Differences in metastatic area reached statistical significance (Wilcoxon-Mann-Whitney exact test) in HTLA-230-pLKO-Slug + imatinib mesylate compared with HTLA230-pLKO-GFP untreated ($P = 0.045$) and in HTLA-230-pLKO-Slug + imatinib mesylate compared with HTLA230-pLKO-GFP + imatinib mesylate ($P = 0.013$; Fig. 5A). Representative sections of adrenals, kidney, and pararenal area of each group are shown in Fig. 5B to E. The involved area was reduced in the untreated (Fig. 5D) and imatinib mesylate–treated (Fig. 5E) HTLA-230-pLKO-Slug groups compared with the untreated (Fig. 5B) and

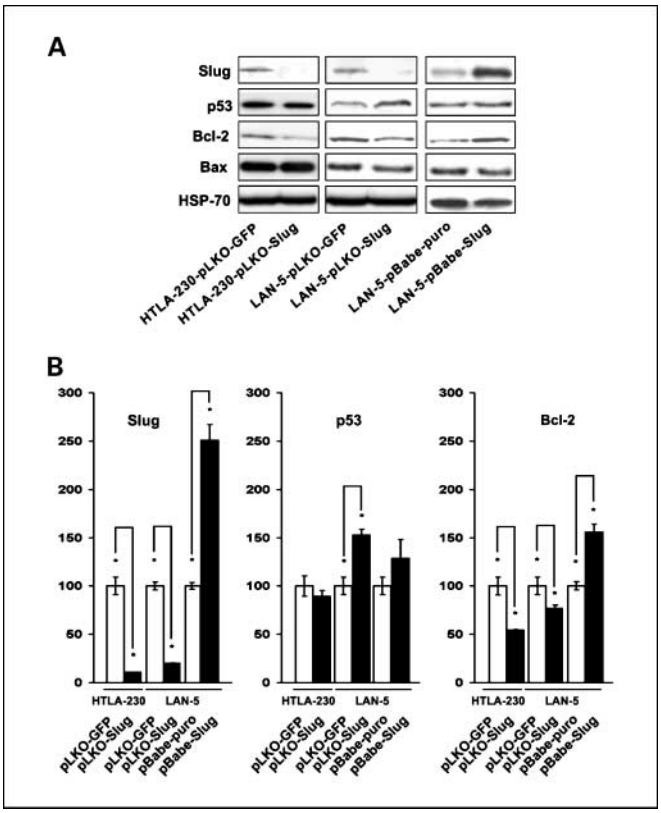

Fig. 3. *A,* Slug, p53, Bcl-2, and Bax immunodetection in Slug-silenced (HTLA-230-pLKO-Slug and LAN-5-pLKO-Slug) and Slug-overexpressing (LAN-5-pBABE-Slug) neuroblastoma cells. Cell extracts were analyzed for expression of the indicated proteins using specific antibodies. The experiment was repeated twice with similar results. *B,* densitometric analysis of Slug, p53, and Bcl-2 levels detected by immunoblotting. Expression level of each protein in controls was set to 100. Levels are reported as percent of control ± SD.

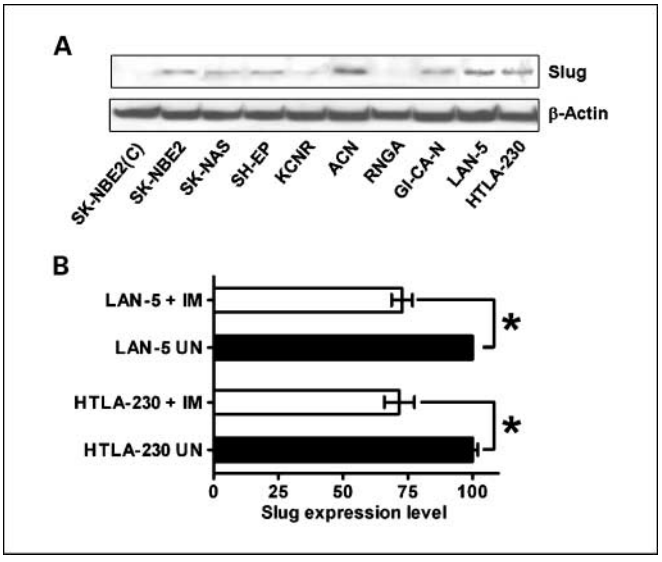

Fig. 2. *A,* Slug is expressed in human neuroblastoma cell lines. Ten cell lines were analyzed for Slug expression by immunoblotting. Filter was stripped and reprobed with anti-β-actin antibody for normalization. The experiment was repeated twice with similar results. *B,* Slug expression measured by quantitative real-time PCR in LAN-5 and HTLA-230 cells untreated or treated with 10 μmol/L imatinib mesylate for 6 h. Expression levels ± SD in untreated cells were taken as 100. *, $P < 0.01$, statistically significant differences (*t* test). Experiments were carried out twice in triplicate.

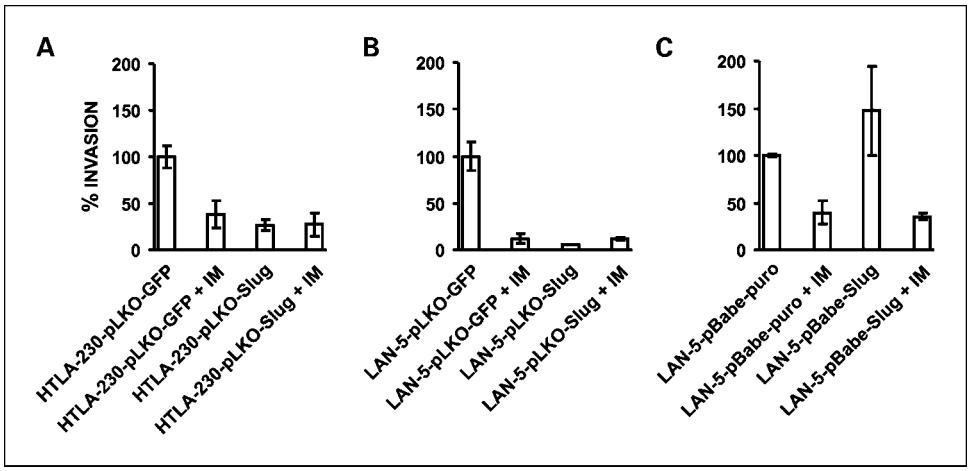

Fig. 4. Slug silencing inhibits (*A* and *B*) Slug overexpression and promotes (*C*) invasion of human neuroblastoma cells in Matrigel-coated invasion chambers. Cells were seeded in the upper chamber in medium supplemented with 5% FCS. Where indicated, cells were treated with imatinib mesylate. After 22 h, cells migrated in the lower chamber were stained and counted. In the lower chamber, medium supplemented with 10% FCS was used as chemoattractant. Invasion of each untreated cell line was set to 100. Results are reported as percent migration ± SD compared with untreated cells. Experiments were carried out twice in triplicate.

imatinib mesylate–treated (Fig. 5C) HTLA230-pLKO-GFP groups. These findings show that silencing of Slug significantly reduces the metastatic burden in a pseudometastatic model of neuroblastoma and that this reduction is more evident following imatinib mesylate treatment of Slug-silenced cells.

Discussion

Effective treatment of metastatic neuroblastoma still remains an unsolved clinical challenge (8). The development of targeted therapies using compounds with a selective mechanism of action and a better toxicity profile compared with conventional cytotoxic drugs paved the way to preclinical studies aimed at using these drugs not only to suppress tumor growth but also to inhibit metastasis. We (16, 17) and others (18–20) reported the activity of imatinib mesylate in inhibiting proliferation of neuroblastoma cells. These results, together with the role of imatinib mesylate targets in the regulation of cell motility (29, 30), encouraged us to also assess whether imatinib mesylate suppressed neuroblastoma cell invasion. *In vitro* assays showed that imatinib mesylate treatment was indeed able to reduce significantly tumor invasiveness. Then, we carried out microarray

Table 2. Flow cytometric analysis of untreated, imatinib mesylate–treated, etoposide-treated, and doxorubicin-treated Slug-silenced neuroblastoma cells

Time of treatment/cell line	Treatment					
	Imatinib mesylate		Etoposide		Doxorubicin	
	% Sub-G_1	*P*	% Sub-G_1	*P*	% Sub-G_1	*P*
Untreated						
LAN-5-pLKO-GFP	0.78	NS	0.78	NS	0.78	NS
LAN-5-pLKO-Slug	0.79		0.79		0.79	
1d						
LAN-5-pLKO-GFP	3.36	NS	8.19	<0.001	14.11	<0.001
LAN-5-pLKO-Slug	3.50		20.18		21.39	
2d						
LAN-5-pLKO-GFP	29.46	<0.001	17.02	<0.001	14.93	<0.001
LAN-5-pLKO-Slug	36.68		22.21		22.65	
3d						
LAN-5-pLKO-GFP	37.07	<0.001	32.33	NS	19.67	<0.001
LAN-5-pLKO-Slug	40.26		32.82		29.41	
Untreated						
HTLA-230-pLKO-GFP	4.86	<0.001	4.86	<0.001	4.86	<0.001
HTLA-230-pLKO-Slug	10.91		10.91		10.91	
1d						
HTLA-230-pLKO-GFP	3.50	<0.001	5.01	<0.001	5.14	<0.001
HTLA-230-pLKO-Slug	16.00		11.57		11.60	
2d						
HTLA-230-pLKO-GFP	23.34	<0.001	13.27	<0.001	15.89	<0.001
HTLA-230-pLKO-Slug	43.80		15.93		18.09	
3d						
HTLA-230-pLKO-GFP	61.36	<0.001	21.70	NS	28.59	NS
HTLA-230-pLKO-Slug	84.23		21.72		28.52	

NOTE: Treatment concentrations were 24 μmol/L imatinib mesylate, 1 μmol/L (LAN-5) and 5 μmol/L (HTLA-230) etoposide, and 1 μg/mL doxorubicin. Flow cytometric analysis was carried out on 2×10^4 cells. Statistical significance was calculated by χ^2 test.
Abbreviation: NS, not significant.

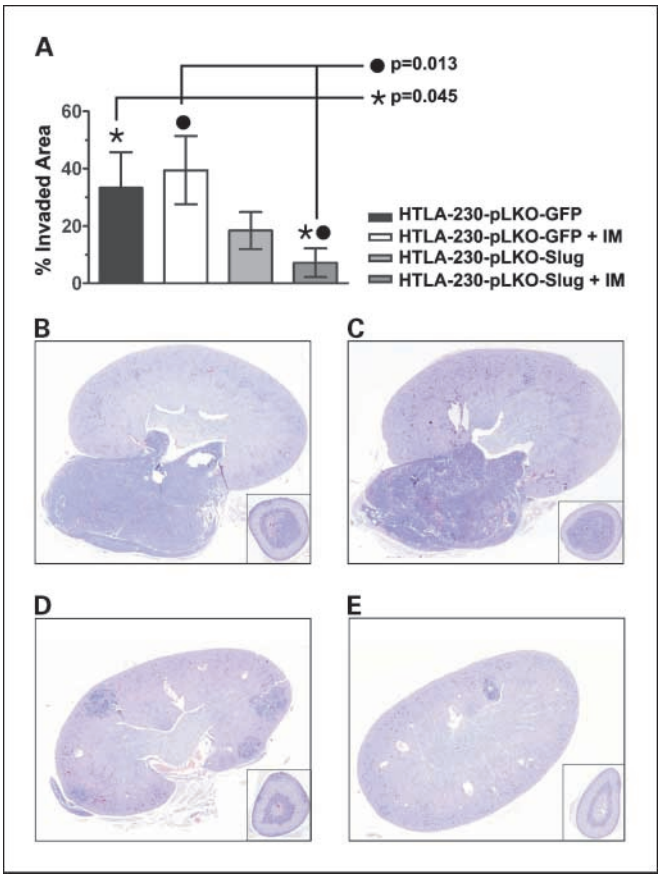

Fig. 5. Effect of Slug silencing and imatinib mesylate treatment in a pseudometastatic model of neuroblastoma *in vivo*. *A,* major sagittal section of kidney, pararenal area, and adrenals of each animal was evaluated for the extent of metastatic invasion using an image analysis program (see Materials and Methods for details). Data are presented as percent of invaded area ± SE. Significant differences in metastatic burden compared with the pLKO-GFP untreated group are indicated. Representative histologic sections of kidney, pararenal area, and adrenals of each group of animals. *B,* HTLA-230-pLKO-GFP untreated. *C,* HTLA-230-pLKO-GFP + imatinib mesylate. *D,* HTLA-230-pLKO-Slug untreated. *E,* HTLA-230-pLKO-Slug + imatinib mesylate.

gene expression analyses of untreated and imatinib mesylate–treated neuroblastoma cells seeded on a layer of extracellular matrix (Matrigel) to identify genes possibly involved in modulating the effects of imatinib mesylate on neuroblastoma invasiveness. The molecular changes necessary for tumor cells to acquire metastatic competence are not yet completely understood. In addition to the important roles during embryonic development, loss of cell adhesion and induction of EMT are also required for tumor progression (3). In fact, induction of EMT represents the first step in the metastatic cascade, allowing cells to delaminate from the primary tumor and to intravasate into lymphatic or blood vessels (13). Activation of Snail, ZEB, and basic helix-loop-helix transcription factors represents one of the molecular switches whereby cells undergoing EMT lose intercellular connections and apico-basal polarity (4). Recently, activation of microRNA-10b by Twist1, an EMT regulator, was also shown to play a role in breast cancer invasion and metastasis (31). Our microarray analysis showed that expression of Slug, a transcriptional repressor whose expression has been associated with mesoderm and migratory neural crest cells undergoing EMT (13), was down-regulated by imatinib mesylate treatment in both cell lines analyzed. Of interest, activation of the c-Kit receptor leads to increased Slug expression in malignant mesothelioma cells (32). c-Kit phosphorylation is down-modulated by imatinib mesylate in neuroblastoma cells (16), although further data indicate that other receptors can be implicated in the effects of imatinib mesylate (19). Thus, although it is conceivable that the Slug down-regulation in neuroblastoma cells may be due, at least in part, to the c-Kit inhibition caused by imatinib mesylate treatment, other receptors inhibited by imatinib mesylate could play a role in Slug down-regulation.

Several experimental data have led to the inclusion of Slug into the Snail family of transcription regulators involved in tumor progression and metastasis (23, 33). In our studies, we found that the knockdown of Slug expression, like imatinib mesylate treatment, inhibited the invasion capability of two neuroblastoma cell lines *in vitro*. In contrast with the marked effect on invasiveness, neither inhibition nor overexpression of Slug significantly affected cell proliferation of the neuroblastoma cell lines in agreement with the data on the proliferation of Slug-silenced melanoma cells (23). Moreover, Slug is also involved in cell survival through the direct or indirect transcriptional regulation of proapoptotic (26, 34) and anti-apoptotic (35) genes. We detected a decrease of Bcl-2 expression in Slug-silenced cells, whereas Bcl-2 levels increased in Slug-overexpressing cells, findings that are in agreement with the antiapoptotic role of Slug in neuroblastoma cells. The enhanced propensity of Slug-silenced neuroblastoma cells to undergo apoptosis is also consistent with the results of imatinib mesylate, etoposide, and doxorubicin treatments *in vitro* and suggests that Slug inhibition could enhance the beneficial effects of proapoptotic drugs even of those (etoposide and doxorubicin) already used in therapeutic protocols.

In tumors, migrating cells leaving the primary mass must counteract anoikis (36), a form of apoptotic cell death triggered by the detachment of cells from the extracellular matrix, to arrive successfully at the final site of metastasis. Thus, the antiapoptotic and proinvasive activities conferred by Slug to neuroblastoma cells *in vitro* could cooperate to promote metastasis competence *in vivo*. Clinical studies have shown that imatinib mesylate treatment is effective in metastatic gastrointestinal stromal tumors through its ability to block c-Kit activity (37). A recent study has also reported that Matrigel invasion of highly aggressive breast carcinoma cells is reduced by imatinib mesylate treatment via the inhibition of activated c-Abl (38). Although it is unknown whether c-Abl is expressed and active in the cell lines used in the present study, we cannot exclude that part of the effects induced by imatinib mesylate may be due to c-Abl inhibition in addition to those dependent on c-Kit (16) or other receptor tyrosine kinases (19). The inhibition of neuroblastoma invasion by imatinib mesylate treatment *in vitro* and the ability of imatinib mesylate to inhibit tyrosine kinases phosphorylation in neuroblastoma cells (16, 19) suggest that this drug may effectively suppress metastasis formation in neuroblastoma.

To investigate whether the combination of Slug knockdown and imatinib mesylate treatment can synergistically reduce the metastatic burden in neuroblastoma, we used a well-established pseudometastatic model in severe combined immunodeficient mice (28). Slug silencing inhibited metastatic growth, although the effects did not reach statistical significance unless Slug-silenced cells were also treated with imatinib mesylate.

Surprisingly, in our *in vivo* model of metastatic neuroblastoma, imatinib mesylate as a single agent was unable to reduce the metastatic burden. This result is in contrast with the findings of the *in vitro* assays, in which imatinib mesylate was indeed able to inhibit invasion. Nevertheless, our data on the inefficacy of imatinib mesylate alone in reducing metastasis *in vivo* are in keeping with the results of the first clinical trial on imatinib mesylate used as single-agent treatment in refractory or relapsed pediatric tumors, including neuroblastoma, which reported little or no activity of imatinib mesylate at a dose of 440 mg/m^2/d (21). A possible explanation for the apparent discrepancy between *in vitro* and *in vivo* results in the present study could be due to inadequate imatinib mesylate concentration at the metastatic sites in the neuroblastoma-injected animals albeit the dose of imatinib mesylate used in this study (200 mg/kg/d) was in the range of those inhibiting neuroblastoma growth in s.c. xenografts (17).

The additive effect of imatinib mesylate in combination with Slug inhibition is unlikely due to a further reduction of Slug levels, because these levels are already undetectable in Slug-silenced cells. Recent data indicate that imatinib mesylate and other small molecules of the same class bind to and modulate the activity of other targets beyond the tyrosine kinases (39). Thus, it is conceivable that imatinib mesylate treatment may affect the expression/activity of other proteins, regulated by established and/or still unknown imatinib mesylate targets, with a role in modulating the metastatic cascade of neuroblastoma cells. This hypothesis is consistent with (*a*) the results of our microarray analysis that shows that imatinib mesylate treatment modulates the expression of several genes, some of which may play a role in neuroblastoma invasion such as Polo-like kinase 2 (40) and activin receptor type II (41), and (*b*) the observation that imatinib mesylate treatment suppresses as the migration of Slug-overexpressing LAN-5 cells (Fig. 4). It should also be taken into account that the *in vitro* invasion ability of SK-N-BE2c cells that do not express Slug (see Fig. 2) was also reduced by imatinib mesylate treatment possibly through a modulation of the activity of other unidentified targets. Also of interest is the observation that c-Abl, whose activation is inhibited by imatinib mesylate, appears to promote the *in vitro* invasion of breast carcinoma cells (38). Even so, in our *in vivo* model, the inhibition of imatinib mesylate targets does not seem sufficient to suppress the development of neuroblastoma metastasis unless coupled with the complete down-regulation of Slug.

In summary, our data have shown for the first time the relevant role of Slug expression in apoptosis, invasion, and metastasis of neuroblastoma cells *in vitro* and *in vivo*. Although metastasis formation in neuroblastoma as well as in other cancers is a highly complex and organized process that consists of multiple interrelated steps (42), Slug seems to play a central role, so that its inhibition significantly decreases, albeit does not eradicate, metastasis formation *in vivo*. Furthermore, the present *in vivo* findings suggest that the combination of Slug down-regulation with imatinib mesylate administration may represent a novel targeted therapy for metastatic neuroblastoma.

Disclosure of Potential Conflicts of Interest

No potential conflicts of interest were disclosed.

References

1. Liotta LA. An attractive force in metastasis. Nature 2001;410:24–5.
2. Steeg PS. Tumor metastasis: mechanistic insights and clinical challenges. Nat Med 2006;12:895–904.
3. Thiery JP, Sleeman JP. Complex networks orchestrate epithelial-mesenchymal transitions. Nat Rev Mol Cell Biol 2006;7:131–42.
4. Peinado H, Olmeda D, Cano A. Snail, Zeb and bHLH factors in tumour progression: an alliance against the epithelial phenotype? Nat Rev Cancer 2007;7:415–28.
5. Deryugina EI, Quigley JP. Matrix metalloproteinases and tumor metastasis. Cancer Metastasis Rev 2006; 25:9–34.
6. Ben-Baruch A. The multifaceted roles of chemokines in malignancy. Cancer Metastasis Rev 2006;25: 357–71.
7. Folkman J. Angiogenesis. Annu Rev Med 2006;57: 1–18.
8. Brodeur GM. Neuroblastoma: biological insights into a clinical enigma. Nat Rev Cancer 2003;3:203–16.
9. Maris JM, Hogarty MD, Bagatell R, Cohn SL. Neuroblastoma. Lancet 2007;369:2106–20.
10. De Bernardi B, Nicolas B, Boni L, et al. Disseminated neuroblastoma in children older than one year at diagnosis: comparable results with three consecutive high-dose protocols adopted by the Italian Co-Operative Group for Neuroblastoma. J Clin Oncol 2003;21: 1592–601.
11. D'Angio GJ, Evans AE, Koop CE. Special pattern of widespread neuroblastoma with a favourable prognosis. Lancet 1971;1:1046–9.
12. Brodeur GM, Seeger RC. Gene amplification in human neuroblastomas: basic mechanisms and clinical implications. Cancer Genet Cytogenet 1986;19: 101–11.
13. Barrallo-Gimeno A, Nieto MA. The Snail genes as inducers of cell movement and survival: implications in development and cancer. Development 2005;132: 3151–61.
14. Druker BJ. Perspectives on the development of a molecularly targeted agent. Cancer Cell 2002;1:31–6.
15. Verweij J, van Oosterom A, Blay JY, et al. Imatinib mesylate (STI-571 Glivec, Gleevec) is an active agent for gastrointestinal stromal tumours, but does not yield responses in other soft-tissue sarcomas that are unselected for a molecular target. Results from an EORTC Soft Tissue and Bone Sarcoma Group phase II study. Eur J Cancer 2003;39:2006–11.
16. Vitali R, Cesi V, Nicotra MR, et al. c-Kit is preferentially expressed in MYCN-amplified neuroblastoma and its effect on cell proliferation is inhibited *in vitro* by STI-571. Int J Cancer 2003;106:147–52.
17. Meco D, Riccardi A, Servidei T, et al. Antitumor activity of imatinib mesylate in neuroblastoma xenografts. Cancer Lett 2005;228:211–9.
18. Beppu K, Jaboine J, Merchant MS, Mackall CL, Thiele CJ. Effect of imatinib mesylate on neuroblastoma tumorigenesis and vascular endothelial growth factor expression. J Natl Cancer Inst 2004;96:46–55.
19. Te Kronnie G, Timeus F, Rinaldi A, et al. Imatinib mesylate (STI571) interference with growth of neuroectodermal tumour cell lines does not critically involve c-Kit inhibition. Int J Mol Med 2004;14:373–82.
20. Rossler J, Zambrzycka I, Lagodny J, Kontny U, Niemeyer CM. Effect of STI-571 (imatinib mesylate) in combination with retinoic acid and γ-irradiation on viability of neuroblastoma cells. Biochem Biophys Res Commun 2006;342:1405–12.
21. Bond M, Bernstein ML, Pappo A, et al. A phase II study of imatinib mesylate in children with refractory or relapsed solid tumors: a Children's Oncology Group study. Pediatr Blood Cancer 2008;50:254–8.
22. Morgenstern JP, Land H. Advanced mammalian gene transfer: high titre retroviral vectors with multiple drug selection markers and a complementary helper-free packaging cell line. Nucleic Acids Res 1990;18: 3587–96.
23. Gupta PB, Kuperwasser C, Brunet JP, et al. The melanocyte differentiation program predisposes to metastasis after neoplastic transformation. Nat Genet 2005;37:1047–54.
24. Raschellà G, Tanno B, Bonetto F, et al. The RB-related gene Rb2/p130 in neuroblastoma differentiation and in B-myb promoter down-regulation. Cell Death Differ 1998;5:401–7.
25. Haupt S, Alsheich-Bartok O, Haupt Y. Clues from worms: a Slug at Puma promotes the survival of blood progenitors. Cell Death Differ 2006;13:913–5.
26. Tribulo C, Aybar MJ, Sanchez SS, Mayor R. A balance between the anti-apoptotic activity of Slug and the apoptotic activity of msx1 is required for the proper development of the neural crest. Dev Biol 2004;275:325–42.
27. Bolos V, Peinado H, Perez-Moreno MA, Fraga MF, Esteller M, Cano A. The transcription factor Slug represses E-cadherin expression and induces epithelial to mesenchymal transitions: a comparison with Snail and E47 repressors. J Cell Sci 2003;116: 499–511.
28. Bogenmann E. A metastatic neuroblastoma model in SCID mice. Int J Cancer 1996;67:379–85.
29. Bellone G, Ferrero D, Carbone A, et al. Inhibition of cell survival and invasive potential of colorectal carcinoma cells by the tyrosine kinase inhibitor STI571. Cancer Biol Ther 2004;3:385–92.
30. Yasuda A, Sawai H, Takahashi H, et al. The stem cell factor/c-kit receptor pathway enhances proliferation and invasion of pancreatic cancer cells. Mol Cancer 2006;5:46.

31. Ma L, Teruya-Feldstein J, Weinberg RA. Tumour invasion and metastasis initiated by microRNA-10b in breast cancer. Nature 2007;449:682–8.

32. Catalano A, Rodilossi S, Rippo MR, Caprari P, Procopio A. Induction of stem cell factor/c-Kit/Slug signal transduction in multidrug-resistant malignant mesothelioma cells. J Biol Chem 2004;279:46706–14.

33. Uchikado Y, Natsugoe S, Okumura H, et al. Slug Expression in the E-cadherin preserved tumors is related to prognosis in patients with esophageal squamous cell carcinoma. Clin Cancer Res 2005;11:1174–80.

34. Wu WS, Heinrichs S, Xu D, et al. Slug antagonizes p53-mediated apoptosis of hematopoietic progenitors by repressing puma. Cell 2005;123:641–53.

35. Bermejo-Rodriguez C, Perez-Caro M, Perez-Mancera PA, Sanchez-Beato M, Piris MA, Sanchez-Garcia I. Mouse cDNA microarray analysis uncovers Slug targets in mouse embryonic fibroblasts. Genomics 2006;87:113–8.

36. Gilmore AP. Anoikis. Cell Death Differ 2005;12 Suppl 2:1473–7.

37. Radford IR. Imatinib. Novartis. Curr Opin Investig Drugs 2002;3:492–9.

38. Srinivasan D, Plattner R. Activation of Abl tyrosine kinases promotes invasion of aggressive breast cancer cells. Cancer Res 2006;66:5648–55.

39. Rix U, Hantschel O, Durnberger G, et al. Chemical proteomic profiles of the BCR-ABL inhibitors imatinib, nilotinib, and dasatinib reveal novel kinase and non-kinase targets. Blood 2007;110:4055–63.

40. Wolf G, Elez R, Doermer A, et al. Prognostic significance of polo-like kinase (PLK) expression in non-small cell lung cancer. Oncogene 1997;14:543–9.

41. Siegel PM, Shu W, Cardiff RD, Muller WJ, Massague J. Transforming growth factor β signaling impairs Neu-induced mammary tumorigenesis while promoting pulmonary metastasis. Proc Natl Acad Sci U S A 2003;100:8430–5.

42. Ara T, DeClerck YA. Mechanisms of invasion and metastasis in human neuroblastoma. Cancer Metastasis Rev 2006;25:645–57.